

Toxicology Research

Accepted Manuscript



This is an *Accepted Manuscript*, which has been through the Royal Society of Chemistry peer review process and has been accepted for publication.

Accepted Manuscripts are published online shortly after acceptance, before technical editing, formatting and proof reading. Using this free service, authors can make their results available to the community, in citable form, before we publish the edited article. We will replace this *Accepted Manuscript* with the edited and formatted *Advance Article* as soon as it is available.

You can find more information about *Accepted Manuscripts* in the [Information for Authors](#).

Please note that technical editing may introduce minor changes to the text and/or graphics, which may alter content. The journal's standard [Terms & Conditions](#) and the [Ethical guidelines](#) still apply. In no event shall the Royal Society of Chemistry be held responsible for any errors or omissions in this *Accepted Manuscript* or any consequences arising from the use of any information it contains.

**Activation of NF- κ B signaling by rare earth neodymium oxide particles-induced
acute lung injury**

Suhua Wang^{1,2}, Yanrong Gao², Lihua Huang², Shanshan Zheng², Chunxia Wang²,
Yanqin Yu², Keqin Xie^{1*}

Author Affiliations:

¹Department of Toxicology, School of Public Health, Shandong University, Jinan,
Shandong 250012, P.R. China

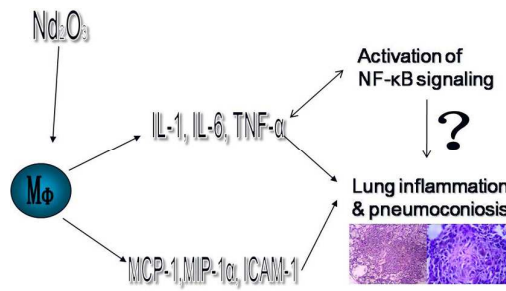
²Department of Environmental and Occupational Health, School of Public Health, Baotou
Medical College, 31 South Construction Street, Baotou, inner Mongolia 014030, P.R.
China

*To whom correspondence should be addressed: Keqin Xie

E-mail: keqinx@sdu.edu.cn

Phone: +86-13853183196

Table of contents entry



The mechanism of activation of NF-κB signaling pathway in Nd₂O₃ exposure induced acute lung inflammation and pneumoconiosis.

Abstract

Neodymium is widely application for industrial materials in the world, and most of the supply is produced in China. Nevertheless, neodymium oxide dust exposure can cause a pronounced lung injury and pneumoconiosis. This study identified the process of Nd₂O₃-induced acute lung injury and explored the activation of NF-κB by employing an Nd₂O₃ instilled rat model. H&E staining, total cell number and total protein amount in BAL fluid revealed that Nd₂O₃ instillation caused a pronounced lung acute injury, which is characterized by the infiltration of inflammatory cells, alveolar septal thickening, fibroblast proliferation and collagen deposition in lung of the rats. Meanwhile, immunoblot analysis and EMSA assay indicated that Nd₂O₃ instillation induced the NF-κB signaling pathway. These results suggest that Nd₂O₃-induced lung acute injury may be regulated by NF-κB signaling pathway, which could be the first *in vivo* mechanistic study of pneumoconiosis, induced by Nd₂O₃, and provide insights for the development of clinical therapeutic strategies to prevent Nd₂O₃-induced pneumoconiosis.

Introduction

Pneumoconiosis is one of the most serious occupational diseases, which is ranked at the top of the 10 leading causes of occupational disease¹. It is a progressive and irreversible fibrogenic lung disease that results in not only human suffering but also unaffordable economic burden. In China, the cumulative number of confirmed pneumoconiosis cases reached 581,377 until 2002. Of those, 139,177 cases (24%) have already died. The economic burden of pneumoconiosis, including direct and indirect costs, reached 0.4% of total GDP in 1999^{2,3}. In addition, there are 12,000-15,000 new cases reported annually (about 70–80% of the total reported cases of occupational diseases) in recent years¹.

China produces over 95% of the world's rare earth elements supply and occupational exposure to them is a known cause of pneumoconiosis^{4,5}. Since rare earth elements have excellent properties of magnetism and electron state, industrial products containing rare earth elements are widely used in a variety of functional materials, such as high-efficiency magnetic materials, solid metal hydrides and catalysts⁶. Experimental toxicology studies have demonstrated that rare earth elements such as yttrium and lanthanum cause pulmonary toxicity in rats^{7,8}. Occupational exposure to cerium (another rare earth element) and its dioxide has been reported to cause pneumoconiosis in workers⁹⁻¹⁸. Therefore, it is necessary to study how the rare earth elements exposure induces lung injury and pneumoconiosis, and to explore potential therapeutic strategies to prevent the progression of lung injury. Among these rare earth elements, neodymium emerges as an important health hazard.

Neodymium is a lustrous, silver-yellow, rare earth metallic element in the lanthanide series within group IIIb of the periodic table. Neodymium oxide (Nd_2O_3), also called neodymia, is widely used for making glass, capacitors, and magnets. However, its toxicity has not been thoroughly investigated. It has been reported that Nd_2O_3 dust are very irritating to the eyes and mucous membranes, with they are moderately irritating to the skin. Its dust inhaling can cause lung embolisms and accumulated exposure damages to the livers¹⁹. And more and more Nd_2O_3 dust exposure induced pneumoconiosis has been reported in these years. Unfortunately, so far there is only one study that focused on the Nd_2O_3 induced cytotoxic effects on the pulmonary macrophages²⁰. To date, no further studies have investigated the systematic mechanism of lung injury after environmental exposure to Nd_2O_3 .

Generally, mineral particles-induced lung injuries are characterized by infiltration of inflammatory cells, alveolar septal thickening, fibroblast proliferation and collagen deposition²¹⁻²³. The lung damage process can be divided into four stages according to histopathological changes^{22, 24}: (1) cellular nodules stage – defined by inflammatory cells infiltration and alveolar septal thickening around the particles inhaled; (2) cellular fibrotic nodules stage – collagen begins to deposit and fibrosis forms across the inflammation sites; (3) fibrotic cellular nodules stage – the number of infiltrated of inflammatory cells decreases and the area of fibrosis formation occupies most part of the inflammation sites; (4) fibrotic nodules stage – the inflammation sites are totally displaced by fibrosis.

Typically, when macrophages in the lungs ingest dust particles, they will set off an inflammatory response by releasing pro-inflammatory cytokines, including tumor necrosis factor α (TNF α), interleukins 1 and 6 (IL1, IL6)^{25, 26}. In turn, these cytokines stimulate fibroblasts to proliferate and secrete collagen around the particle^{27, 28}. In addition, the macrophages that ingested the particles also produce chemokines such as MCP-1, MIP-1 α , and ICAM-1, which are crucial for the inflammatory response²⁹. MCP-1 (monocyte chemoattractant protein-1) is a small cytokine that belongs to the CC chemokine family that recruits monocytes, memory T cells, and dendritic cells to the sites of inflammation³⁰. MIP-1 α (macrophage inflammatory protein-1 α) belongs to the family of chemotactic cytokines; it activates granulocytes (neutrophils, eosinophils and basophils) and induces the synthesis and release of pro-inflammatory cytokines such as IL1, IL6 and TNF α from fibroblasts and macrophages³¹. ICAM-1 (intercellular adhesion molecules 1) can bind with LFA-1 (leucocyte function-associated molecule 1) on resting T cells to activate them and induce their proliferation³².

NF- κ B (nuclear factor kappa-light-chain-enhancer of activated B cells) is a transcription factor found in almost all cell types that is involved in the cellular responses to stimuli such as stress, cytokines, free radicals, ultraviolet irradiation, oxidized LDL, and bacterial or viral antigens. In unstimulated cells, the NF- κ B dimers are sequestered in the cytoplasm by I κ B (inhibitor of κ B). When the NF- κ B signaling is activated, a kinase called the I κ B kinase β (IKK β) will be phosphorylated, which in turn phosphorylates two serine residues located in a regulatory domain of I κ B. The phosphorylated I κ B is then degraded by the

proteasome, allowing the activated NF- κ B to translocate to the nucleus to induce the transcription of pro-inflammation cytokines such as IL1, IL6, and TNF α ^{33, 34}.

In this study, we investigated the process of Nd₂O₃-induced lung injury and explored the activation of NF- κ B signaling by employing an Nd₂O₃ instilled rat model. We found that Nd₂O₃ instillation caused a pronounced lung injury, characterized by the infiltration of inflammatory cells, alveolar septal thickening, fibroblast proliferation and collagen deposition in the rats. We also identified that the NF- κ B signaling pathway was activated in the Nd₂O₃-induced lung injury. These results suggest that Nd₂O₃-induced lung injury may be regulated by NF- κ B signaling pathway, which could be the first *in vivo* mechanistic study of pneumoconiosis, induced by Nd₂O₃, and provide insights for the development of clinical therapeutic strategies to prevent Nd₂O₃-induced pneumoconiosis.

Results

Nd₂O₃ instillation leads to lung pathological changes.

To investigate the effects of Nd₂O₃-induced lung injury, rats were instilled with Nd₂O₃ and the lung tissues were observed to monitor pathological changes. H&E staining revealed that infiltration of inflammatory cells and alveolar septal thickening were significantly increased in the lungs of rats in Nd₂O₃ group as early as day 3 post-instillation, compared to the lungs of rats in control group (Figure1, A1-4). Meanwhile, irregular cellular nodules were observed with Nd₂O₃ instillation at day 3 (Figure1, A3). This inflammatory response was persistent and continuously increased, since at day 7 post instillation in Nd₂O₃ group (Figure1, B1-4) we detected more and larger cellular nodules compared to day 3 (Figure2, A3). At day 14, the level of lung inflammation induced by Nd₂O₃ was even more exacerbated (Figure1, C3-4), and obvious fibrosis began to form across the cellular nodules, which suggests that the cellular nodules were transformed into cellular fibrotic nodules. In addition, the amount and size of cellular nodules also increased (Figure1, C4). At day 21, the inflammation in the lungs of rats in Nd₂O₃ group began to decrease (Figure1, D3-4). However, no increase in the number of cellular fibrotic nodules was observed but the size of preexisting ones kept growing, compared with day 14 with Nd₂O₃ instillation (Figure1, D3-4). At day 28, the inflammation of the lungs with Nd₂O₃ instillation was evidently resolved (Figure1, E1-4) and most of the cellular fibrotic nodules had become mostly fibrotic at this time point (Figure1, E3-4). These results indicated that Nd₂O₃ instillation caused a pronounced lung inflammation, which is a process from cellular nodules to fibrotic nodules.

Total cell number and total protein amount in BAL fluid were increased in the lungs of rats with Nd₂O₃ intratracheal instillation.

To further evaluate the levels of inflammation and injury to the lungs of rats after Nd₂O₃ instillation, total cell number and total protein in the BAL fluid was measured. In the Nd₂O₃ group, we observed a trend for increase in the total cell number in BAL fluid from day 3 to day 28 post instillation (Figure 2A), compared to the control group. Nevertheless, at day 14 we observed an unexpected decrease in the total cell number in BAL fluid that was not consisted with the trend we observed in all other time points (Figure 2A). This value was lower than that observed at days 7 or 21, but still higher than the value observed at day 3 after Nd₂O₃ instillation.

Next, the level of total protein in BAL fluid was measured, and we observed a trend that was consistent with the total cell number. With Nd₂O₃ instillation, more total protein was detected in BAL fluid compared to the control group, and the values also increased in a time dependent manner (Figure 2B). Similarly, the level of total protein in BAL fluid from Nd₂O₃ group was significantly decreased at day 14 (Figure 2B). These data suggest that Nd₂O₃ instillation can induce cell infiltration to the lung, which is consistent with the histopathological changes, and cause increased alveolar leakage.

Nd₂O₃ instillation increased the levels of pro-inflammatory cytokines in BAL fluid.

The levels of the pro-inflammatory cytokines (IL1, IL6, and TNF α) were next evaluated by

ELISA assay in the BAL fluid to further evaluate the effect of Nd₂O₃ on lung inflammation. Compared to the control group, the levels of IL1 and TNF α secretion in BAL fluid from the lungs of rats with Nd₂O₃ instillation were significantly increased (Figure 3A and 3C). The levels of IL6 secretion in BAL fluid from the lungs of rats with Nd₂O₃ instillation also increased although they did not reach statistical significance (Figure 3B). This data suggested Nd₂O₃ instillation induced pro-inflammatory cytokines secretion, which could activate more macrophages, as well as stimulate fibroblasts to proliferate and secrete collagen around the Nd₂O₃ particle.

Nd₂O₃ instillation increased the level of inflammatory chemokines in BAL fluid.

In addition to the cytokine measurements, we assessed the levels of chemokines as an indirect measurement of inflammatory cells recruitment to the lung. In the rats that were instilled with Nd₂O₃, we observed a trend towards higher induction of the inflammatory chemokines (MCP-1, MIP-1 α , and ICAM-1) compared with the control group. However, only the level of MCP-1 and MIP-1 α showed significant increases at day 28, compared to the control group (Figure 4). These results demonstrated that Nd₂O₃ instillation induced inflammatory chemokines secretion, which resulted in more inflammatory cells recruitment to the lung tissue.

Nd₂O₃ instillation induced the NF- κ B signaling.

Since the levels of the pro-inflammatory cytokines of IL1, IL6, and TNF α were induced after Nd₂O₃ instillation, we decided to look into the NF- κ B signaling pathway since these

are all targets of this transcription factor. Total protein was extracted from lung tissues harvested at the indicated time points post instillation. The lysates were subjected to immunoblot analysis to detect expression of the NF- κ B P65 subunit, phosphorylation of P65 (p-P65) as a marker of NF- κ B activation, and p-IKK β as a marker for inactivation of the repressor. Activation of the NF- κ B pathway was indicated by an increased p-P65 while the total protein levels of P65 did not change in the Nd₂O₃ group (Figure 5A). The levels of p-P65 peaked at day 14 and then slowly decreased at day 28 in the Nd₂O₃ group. The levels of p-IKK β were induced by Nd₂O₃ instillation in a similar manner as they peaked at day 14 and then decreased by day 28 (Figure 5A). No changes were observed in the p-P65, P65, or p-IKK β in the control group (Figure 5A). The changes in the protein levels were quantified and adjusted to the expression of β -actin to further verify protein induction (Figure 5B).

Then, to continue the characterization of the activation of the NF- κ B signaling pathway, the nuclear protein was extracted from the lung tissues of rats in control group (day 3 and day 7, n=2) and Nd₂O₃ group (day 3, 7, 14, 21 and 28, n=4) for an EMSA assay. Since the immunoblotting revealed there are no changes in NF- κ B P65 or IKK β phosphorylation in the control group (Figure 5), we only included two samples from two time points as controls. Consistent with the results from Figure 5, the nuclear translocation of NF- κ B P50/P65 was induced in the lung tissue of rats after Nd₂O₃ instillation. Importantly, as seen previously, the translocation of NF- κ B P50/P65 increased at day 3, and peaked at day 14, then began to decrease at day 21. Together with the histopathological changes,

these results indicated that NF- κ B signaling pathway was playing an important role in Nd₂O₃ instillation induced lung inflammation.

Nd₂O₃ dust intratracheal instillation induced histopathological changes in the lungs of rats along with the activation of NF- κ B signaling pathway in a dose-dependent manner.

To further confirm the activation of NF- κ B signaling pathway in the process of Nd₂O₃-induced lung damage, the rats were intratracheal instilled with different doses of Nd₂O₃ for 14 days. The lung tissues were observed to investigate pathological changes and the activation of NF- κ B signaling pathway post instillation. H&E staining revealed that infiltration of inflammatory cells and alveolar septal thickening were significantly increased in the lungs of rats in Nd₂O₃ group as low as 25 mg/kg intratracheal instillation (Figure7, B1-2) compared to the lungs of rats without Nd₂O₃ administrated (Figure7, A1-2). This inflammatory response and fibrosis across the cellular nodules were persistent and continuously increased in a dose-dependent manner (Figure7, A-E). Total protein was extracted from lung tissues harvested with different doses of Nd₂O₃ instillation at day 14 post instillation. The lysates were subjected to immunoblot analysis to detect expression of the NF- κ B P65 subunit, p-P65 and p-IKK β . Activation of the NF- κ B pathway was indicated by a dose-dependent increased p-P65 while the total protein levels of P65 did not change (Figure 7F). The levels of p-IKK β were induced by Nd₂O₃ instillation in a similar manner (Figure 7F). The changes in the protein levels were quantified and adjusted to the expression of β -actin to further verify protein induction (Figure 7G).

Discussion

Currently, neodymium is widely application in the industrial material, most of which supply is produced in China. In addition, exposure to Nd_2O_3 induced pneumoconiosis is a progressive and irreversible fibrogenic lung disease, and it results in not only human suffering but also unaffordable economic burden. Therefore, lung injury and pneumoconiosis induced by Nd_2O_3 have been regarded as seriously environmental and occupational problems. Therefore, it is very important to clarify the health effects with environmental and occupational exposed to Nd_2O_3 dust. In this study, we originally explored the activation of NF- κ B signaling pathway in Nd_2O_3 induced acute lung injury by using Nd_2O_3 instillation rat model. (1) We found that Nd_2O_3 instillation caused pronounced lung damage, which was characterized by the infiltration of inflammatory cells, alveolar septal thickening and fibrosis formation. (2) We identified the process of the lung injury in the rats with Nd_2O_3 instillation. (3) We identified the NF- κ B signaling pathway was activated in the Nd_2O_3 induced lung injury.

First, compared with other mineral particles-induced lung injuries, the process of lung acute injury induced by Nd_2O_3 instillation can also be divided into four stages according to histopathological changes: (1) cellular nodules stage; (2) cellular fibrotic nodules stage; (3) fibrotic cellular nodules stage; (4) fibrotic nodules stage. But we found that in our Nd_2O_3 instillation rat model, the fibrosis formation is much earlier. Dr. Chen and his partners reported the fibrosis formation could be observed at day 21 in their silicosis induced by

silica dioxide model³⁵, while in our study, we find that the fibrosis formation was clearly observed at day 14. In this study, we identified the NF- κ B signaling pathway was activated in the Nd₂O₃ induced acute lung injury. When macrophages in the lungs ingested Nd₂O₃ dust, NF- κ B signaling pathway in the macrophages was activated as early as day 3, peaked at day14 (Figure 5-6). IKK β was phosphorylated (Figure 5), which in turn phosphorylates two serine residues located in a regulatory domain of I κ B. After phosphorylated I κ B degraded by the proteasome, the phosphorylated P65 translocated to the nucleus, which induced the transcription of pro-inflammation cytokines (IL1, IL6, and TNF α) and chemokines (MCP-1, MIP-1 α , and ICAM-1) as early as day 3 (Figures 3-4). These cytokines released caused more inflammatory cells recruited into the lung inflammatory sites, fibrosis activation and collagen deposition (Figure 1). And along with more NF- κ B signaling pathway activated, the inflammation induced by dust would be more pronounced. These data indicated that it would be very important to treat the acute injury induced by Nd₂O₃ exposure, which can effectively limit the following lung fibrosis formation and suppress the pneumoconiosis.

Second, we clarified the process of lung injury in Nd₂O₃ instillation rat model. Histopathological changes revealed that the Nd₂O₃ induced lung inflammation led to a heavy lung fibrosis (Figure 1, E3-4). In the early stage, lung macrophages with Nd₂O₃ particles ingested will secrete the pro-inflammatory cytokines (IL1, IL6 and TNF α) (Figure 3) and chemokines (MCP-1, MIP-1 α and ICAM-1) (Figure 4), to activate other macrophages and recruit other inflammatory cells (neutrophil, T cells, dendritic cells and

so on) into the inflammatory sites, which caused the formation of cellular nodules. Dr. Long-Ping Wen and his partners found that nano neodymium oxide could cause cell death through massive vacuolization and autophagy³⁶. Therefore, when the macrophages died, the particles will be released, and re-ingested by other macrophage. Followed by that, more and more inflammatory cells will be recruited in the lung tissues (Figure 2A). Besides that, the cytokines set off by the macrophages can also activate the fibroblast to proliferate and collage deposit, resulting in the particles encircled into the collagen and separated from the macrophages and other inflammatory cells. With less macrophages been activated, the infiltration of inflammatory cells will decrease and the fibrotic nodules are formed (Figure 1, A3-E3, A4-E4).

Third, to further confirm the infiltration of inflammatory cells in the Nd₂O₃ group and investigate lung damage, we detected the total cell number and the total protein in the BAL fluid. We found both of them were dramatically increased in Nd₂O₃ group, which indicated the serious of lung inflammation and damage. And unexpected, at day 14, both the total cell number and total protein amount in the BAL fluid was dramatically decreased compare to day 7 in Nd₂O₃ group. These may be because the instilled Nd₂O₃ also induced the apoptosis or autophagic cell death of inflammatory cells. So far, a lot of *in vitro* and *in vivo* studies have reported that nano particles generate ROS lead to oxidative stress causing cell death³⁷⁻⁴⁰. Particularly, Dr. A. Srinicas and his partners have reported that acute inhalation exposure of CeO₂ resulted in a significant decrease in cell viability of BAL fluid up to 14 days post inhalation exposure period, and the levels of LDH activity in BALF

were increased, suggesting that nano particles induced cells apoptosis in BAL fluid, which is consistent with our study⁴¹. Beyond that, there is another possibility that nano particles promote acute lung injury by inducing autophagic cell death through the Akt-TCS2-mTOR signaling pathway⁴². And there is one group also reported that neodymium can induce autophagic cell death too³⁶. At day 21, the total cell number and total protein amount increased again. It may be because the collagen deposited and encircled the Nd₂O₃ particles into it, which cause the separation of the particles away from the inflammatory cells (Figure 1). However, NF-κB signaling pathway was still activated (Figure 5), and the P50/P65 subunits translocated into the nucleus. Then, pro-inflammatory cytokines and chemokines were transcribed and secreted to recruit and activate even more inflammatory cells in the lung. Because the particles that can be ingested by the macrophages were decreased, the level of the activation of NF-κB signaling also decreased from day 14 (Figure 5 and 6).

In summary, our study provides proof-of-concept experimental evidence that NF-κB signaling pathway plays an important role in the Nd₂O₃ induced lung acute damage. H&E staining, total cell number and total protein amount in BAL fluid revealed that Nd₂O₃ instillation caused a pronounced lung injury, which is characterized by the infiltration of inflammatory cells, alveolar septal thickening, fibroblast proliferation and collagen deposition in lung of the rats. Meanwhile, immunoblot analysis and EMSA assay indicated that Nd₂O₃ instillation induced the NF-κB signaling pathway. These results suggest that Nd₂O₃-induced lung injury may be regulated by NF-κB signaling pathway, which could be

the first *in vivo* mechanistic study of pneumoconiosis, induced by Nd_2O_3 , and provide insights for the development of clinical therapeutic strategies to prevent Nd_2O_3 -induced pneumoconiosis. In the future, we will focus on two related studies: (1) identify the effective and specific NF- κ B inhibitors to inhibit its activity for intervention of pneumoconiosis associated with exposure to environmental Nd_2O_3 exposure; (2) explore the most fitting curing time to prevent the procession of pneumoconiosis.

Experimental

Chemicals

Nd₂O₃ was purchased from Ruixing Rare Earth Smelting Factory. Tested by Baotou Rare Earth Institute (OD value is 0.11 μm, 97% is less than 0.29 μm, and purity: 99%). Pentobarbital sodium, Eosin, Hymatoxylin and Cell lysate buffer and Enzyme-linked immunosorbent assay (ELISA) kits for IL1, IL6, TNFα, MCP-1, MIP-1α, and ICAM-1 were purchased from Thermo Scientific. Nonradioactive EMSA Probe Biotin Labeled Kit for NF-κB p-P65/P65 activity was purchased from Beijing HIO Biological Technology Co. Ltd. RIPA buffer, 30% Acrylamide solution, 10% Ammonium persulfate (APS), TEMED and 10% SDS were purchased from Sigma-Aldrich.

Animals and treatments

Sprague-Dawley rats weighing 250-350g were purchased from National Institutes for Food and Drug Control. All animals were housed in a specific-pathogen-free environment and received water and food ad libitum. Animals received humane care in compliance with the Guidance Suggestions for the Care and Use of Laboratory Animals, formulated by the Ministry of Science and Technology of the People's Republic of China. Experiment procedures were approved by the Animal Care and Use Committee of Baotou Medical College. For the time dependent studies, rats were randomly allocated into 2 groups: control (PBS) and Nd₂O₃ (100 mg/kg in PBS) intratracheal instillation (n = 35 per group). Rats were sacrificed for lung tissue and BAL collection at 5 different time points: Day 3, 7, 14, 21, and 28 post-instillation (n = 7 per time point). All rats survived intratracheal

instillation. For the dose dependent studies, rats were randomly allocated into 5 groups: control (PBS) and Nd₂O₃ (25 mg/kg, 50 mg/kg, 100 mg/kg and 150 mg/kg in PBS) intratracheal instillation. Rats were sacrificed for lung tissue at day 14 post-instillation (n = 7 per time point). All rats survived intratracheal instillation.

BAL and lung tissue collection

Rats were euthanized and BAL fluid was obtained by lavaging the lung with 5 ml PBS. The lungs were isolated by carefully opening the thoracic cavity. The BAL fluid was centrifuged at 1500 rpm for 15 minutes at 4 °C. Cell pellets were pooled, washed, and resuspended in PBS. Total cell counts were determined using hemocytometer. The means ± SEM was obtained from 7 rats in the same group. The supernatant was stored at - 80 °C until used for ELISA assay. Lungs were then collected and divided into two parts: one part was frozen in liquid nitrogen for protein analysis. The other part was fixed in 10% buffered formalin to be embedded in paraffin.

Histological analysis

The paraffin embedded tissue was cut into 5 µm sections for histological analysis. The sections were stained with hematoxylin and eosin (H&E) for pathological examination. A representative pathological image for each group was shown at the indicated time points.

ELISA of cytokines in BAL fluid

The ELISA was used to detect the levels of cytokines in the BAL according to the

manufacturer's instructions. Briefly, the plate was coated with 100 μ l capture antibody in coating buffer per well and incubated overnight at room temperature. The plate was washed with 250 μ l wash buffer, blocked with 200 μ l of the assay diluents, and incubated at room temperature for 1 hour. A 100 μ l of the BAL fluid was added and incubated at room temperature for 2 hours. 100 μ l detection antibody was then added to each well and incubated for 1 hour at room temperature. Subsequently, 100 μ l avidin-HRP was added and the plate was incubated for 30 minutes at room temperature. 100 μ l of the substrate solution was added to each well and incubated for 15 minutes at room temperature and then 50 μ l of the stop solution was added to stop the reaction. The plate was then read at 450nm and analyzed. The ELISA was performed in triplicate. Serial dilutions of standards were also used to obtain a standard curve.

Antibodies, and immunoblot analysis.

Antibodies for p-IKK β , p-P65, P65, and β -actin were purchased from Santa Cruz. The rat lung tissues were lysed in RIPA buffer. After sonication, lysates were electrophoresed through an SDS-polyacrylamide gel, transferred to membranes and subjected to immunoblot analysis with the indicative antibodies. Briefly, the membranes were incubated overnight at 4 $^{\circ}$ C with primary antibodies. After the membranes were washed 3 times with Tris buffer containing 0.1% tween-20 (TBST), following by secondary antibodies incubation for 1 hour at room temperature. The relative intensity of the bands was quantified using Image J free software.

Non-Radioactive Electrophoretic mobility shift assay (EMSA) for NF- κ B

The EMSA was used according to the manufacturer's instructions. Briefly, the nuclear protein extraction was performed as described⁴³ and the obtained nuclear extract supernatant was stored at -80 °C. 2 μ g nuclear protein was used to bind with poly (dI:dC) probe sequence [NF- κ B (5'-AGTTGAGGGGACTTTCCCAGG C-3')] in binding reaction, or with together with cold oligonucleotides in competing reaction for 20 minutes. Then the samples were subjected to an electrophoresis and electro-transfer. After the transfer, remove the nylon-membrane and place it in a vacuum oven at 80 °C for 2 hours. The membrane was developed and the relative intensity of the bands was quantified using Image J online free software.

Statistics

Results are presented as the mean \pm SEM (n = 7). Statistical tests were performed using SPSS 13.0. Unpaired Student's t-tests were used to compare the means of two groups. *p* < 0.05 was considered to be significant.

Conclusion

This study identified the process of Nd₂O₃-induced lung injury and explored the regulation of NF-κB by employing an Nd₂O₃ instilled rat model. H&E staining, total cell number and total protein amount in BAL fluid revealed that Nd₂O₃ instillation caused a pronounced lung injury, which is characterized by the infiltration of inflammatory cells, alveolar septal thickening, fibroblast proliferation and collagen deposition in lung of the rats. Meanwhile, immunoblot analysis and EMSA assay indicated that Nd₂O₃ instillation induced the NF-κB signaling pathway. These results suggest that Nd₂O₃-induced lung injury may be regulated by NF-κB signaling pathway, which could be the first *in vivo* mechanistic study of pneumoconiosis, induced by Nd₂O₃, and provide insights for the development of clinical therapeutic strategies to prevent Nd₂O₃-induced pneumoconiosis.

Acknowledgements

This work was supported by grants: National Natural Science Foundation of China 81260426 and Natural Science Foundation of Inner Mongolia 2012MS1102.

Competing financial interests

The authors declare no competing financial interests.

Reference

1. Y. Liang and Q. Xiang, *Toxicology*, 2004, **198**, 45-54.
2. Y. X. Liang, Z. Su, W. A. Wu, B. Q. Lu, W. Z. Fu, L. Yang and J. Y. Gu, *Regul Toxicol Pharmacol*, 2003, **38**, 112-123.
3. Y. X. Liang, O. Wong, H. Fu, T. X. Hu and S. Z. Xue, *Occup Environ Med*, 2003, **60**, 383-384.
4. , China's Rare Earth Dominance, Wikinvest, Retrieved on 11 Aug 2010.
5. H. J. Haxel G, Orris J, in *Reston (VA): United States Geological Survey. USGS Fact Sheet: 087-02*, 2006.
6. T. Toya, A. Takata, N. Otaki, M. Takaya, F. Serita, K. Yoshida and N. Kohyama, *Industrial health*, 2010, **48**, 3-11.
7. K. T. Suzuki, E. Kobayashi, Y. Ito, H. Ozawa and E. Suzuki, *Toxicology*, 1992, **76**, 141-152.
8. S. Hirano, N. Kodama, K. Shibata and K. T. Suzuki, *Toxicol Appl Pharmacol*, 1990, **104**, 301-311.
9. M. H. Husain, J. A. Dick and Y. S. Kaplan, *The Journal of the Society of Occupational Medicine*, 1980, **30**, 15-19.
10. E. Sabbioni, R. Pietra, P. Gaglione, G. Vocaturo, F. Colombo, M. Zanoni and F. Rodi, *Sci Total Environ*, 1982, **26**, 19-32.
11. G. Vocaturo, F. Colombo, M. Zanoni, F. Rodi, E. Sabbioni and R. Pietra, *Chest*, 1983, **83**, 780-783.
12. F. Heuck and R. Hoschek, *The American journal of roentgenology, radium therapy, and nuclear medicine*, 1968, **104**, 777-783.
13. F. Sulotto, C. Romano, A. Berra, G. C. Botta, G. F. Rubino, E. Sabbioni and R. Pietra, *Am J Ind Med*, 1986, **9**, 567-575.
14. Y. Murata, N. Sato, A. Kurashima, M. Yamagishi and T. Yamato, *Nihon Kyobu Shikkan Gakkai Zasshi*, 1985, **23**, 699-703.
15. P. M. Waring and R. J. Watling, *Med J Aust*, 1990, **153**, 726-730.
16. J. C. Pairon, F. Roos, Y. Iwatsubo, X. Janson, M. A. Billon-Galland, J. Bignon and P. Brochard, *Occup Environ Med*, 1994, **51**, 195-199.
17. J. W. McDonald, A. J. Ghio, C. E. Sheehan, P. F. Bernhardt and V. L. Roggli, *Modern pathology : an official journal of the United States and Canadian Academy of Pathology, Inc*, 1995, **8**, 859-865.
18. S. Porru, D. Placidi, C. Quarta, E. Sabbioni, R. Pietra and S. Fortaner, *J Trace Elem Med Biol*, 2001, **14**, 232-236.
19. <http://en.wikipedia.org/wiki/Neodymium>.
20. R. J. Palmer, J. L. Butenhoff and J. B. Stevens, *Environ Res*, 1987, **43**, 142-156.
21. J. C. Bonner, *Toxicol Pathol*, 2007, **35**, 148-153.
22. J. D. Byrne and J. A. Baugh, *McGill journal of medicine : MJM : an international forum for the advancement of medical sciences by students*, 2008, **11**, 43-50.
23. V. Rabolli, S. Lo Re, F. Uwambayinema, Y. Yakoub, D. Lison and F. Huaux, *Toxicol Lett*, 2011, **203**, 127-134.
24. W. A. Wuyts, C. Agostini, K. M. Antoniou, D. Bouros, R. C. Chambers, V. Cottin, J. J. Egan, B. N. Lambrecht, R. Lories, H. Parfrey, A. Prasse, C. Robalo-Cordeiro, E. Verbeken, J. A. Verschakelen, A. U. Wells and G. M. Verleden, *Eur Respir J*, 2013, **41**, 1207-1218.
25. J. E. Losa Garcia, F. M. Rodriguez, M. R. Martin de Cabo, M. J. Garcia Salgado, J. P. Losada, L. G.

- Villaron, A. J. Lopez and J. L. Arellano, *Mediators Inflamm*, 1999, **8**, 43-51.
26. G. B. Toews, *The European respiratory journal. Supplement*, 2001, **34**, 3s-17s.
27. K. Zhang and S. H. Phan, *Biological signals*, 1996, **5**, 232-239.
28. F. Ogushi, *Nihon Ika Daigaku zasshi*, 1996, **63**, 391-394.
29. N. M. Bless, M. Huber-Lang, R. F. Guo, R. L. Warner, H. Schmal, B. J. Czermak, T. P. Shanley, L. D. Crouch, A. B. Lentsch, V. Sarma, M. S. Mulligan, H. P. Friedl and P. A. Ward, *J Immunol*, 2000, **164**, 2650-2659.
30. M. A. van Zoelen, M. I. Verstege, C. Draing, R. de Beer, C. van't Veer, S. Florquin, P. Bresser, J. S. van der Zee, A. A. te Velde, S. von Aulock and T. van der Poll, *Mol Immunol*, 2011, **48**, 1468-1476.
31. D. N. Cook, *J Leukoc Biol*, 1996, **59**, 61-66.
32. R. Seth, F. D. Raymond and M. W. Makgoba, *Lancet*, 1991, **338**, 83-84.
33. R. Schreck, K. Albermann and P. A. Baeuerle, *Free radical research communications*, 1992, **17**, 221-237.
34. H. R. Wong and J. R. Wispe, *Am J Physiol*, 1997, **273**, L1-9.
35. F. Liu, J. Liu, D. Weng, Y. Chen, L. Song, Q. He and J. Chen, *PloS one*, 2010, **5**, e15404.
36. Y. Chen, L. Yang, C. Feng and L. P. Wen, *Biochem Biophys Res Commun*, 2005, **337**, 52-60.
37. A. Nel, T. Xia, L. Madler and N. Li, *Science*, 2006, **311**, 622-627.
38. N. Li, T. Xia and A. E. Nel, *Free Radic Biol Med*, 2008, **44**, 1689-1699.
39. E. J. Park, J. Yi, K. H. Chung, D. Y. Ryu, J. Choi and K. Park, *Toxicol Lett*, 2008, **180**, 222-229.
40. E. J. Park, J. Choi, Y. K. Park and K. Park, *Toxicology*, 2008, **245**, 90-100.
41. A. Srinivas, P. J. Rao, G. Selvam, P. B. Murthy and P. N. Reddy, *Toxicol Lett*, 2011, **205**, 105-115.
42. C. Li, H. Liu, Y. Sun, H. Wang, F. Guo, S. Rao, J. Deng, Y. Zhang, Y. Miao, C. Guo, J. Meng, X. Chen, L. Li, D. Li, H. Xu, H. Wang, B. Li and C. Jiang, *Journal of molecular cell biology*, 2009, **1**, 37-45.
43. A. C. Poletto, D. T. Furuya, A. David-Silva, P. Ebersbach-Silva, C. Lellis Santos, M. L. Correa-Giannella, M. Passarelli and U. F. Machado, *Mol Cell Endocrinol*, 2015, **401**, 65-72.

Figure legends

Figure 1. Histopathology changes in the lungs of rats with Nd₂O₃ dust intratracheal (100 mg/kg in PBS) instillation. A1-4, Day 3; B1-4, Day 7; C1-4, Day 14; D1-4, Day 21; E1-4, Day 28. A1-E1, Control group, 100x; A2-E2, Control group, 400x; A3-E3, Nd₂O₃ group, 100x; A4-E4, Nd₂O₃ group, 400x. (n = 7, a representative image of the lung tissue from each group is shown). Scale bar for 100x: 150 μm; 400x: 40 μm.

Figure 2. Total cell number and total protein amount in BAL increased in the lungs of rats after rare earth Nd₂O₃ dust intratracheal instillation. (A) Total cell number in BAL; (B) Total protein amount in BAL of the rat lungs harvested from indicated time points.

Figure 3. Inflammation cytokines in BAL induced in the lungs of rats with the rare earth Nd₂O₃ dust intratracheal instillation. (A) IL1; (B) IL6; (C), TNFα.

Figure 4. Chemokines in BAL increased in the lungs of rats intratracheally instilled with the rare earth Nd₂O₃ dust. (A) MCP-1; (B) MIP-1α; (C) ICAM-1.

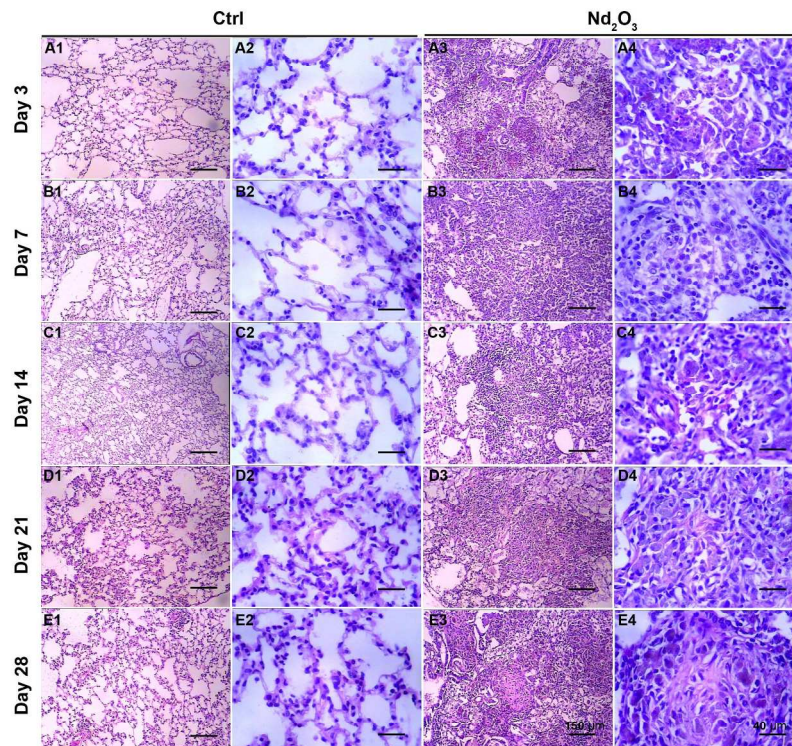
Figure 5. NF-κB signaling pathway induced in the lungs of rats with the rare earth Nd₂O₃ dust intratracheal instillation. (A) Lung tissue lysates from Ctrl group rats and Nd₂O₃ rats were subjected to immunoblot analysis with the indicated antibodies (n = 7, each lane is an individual rat lung tissue lysate from indicated time point, and a representative western blot data is shown). (B) The intensity of bands was quantified and the relative ratio of

p-P65/P65/ β -actin and p-IKK β / β -actin were plotted. Results are expressed as mean \pm SEM (n = 7) (*p<0.05 Day 3 group vs. other treatment groups).

Figure 6. NF- κ B P50/P65 activity increased in the lungs of rats administered with the rare earth Nd₂O₃ dust. (A) Lung tissue lysates from Ctrl groups (Day 3, 7) and Nd₂O₃ groups (Day 3, 7, 14, 21 and 28) were subjected to EMSA assay to detect the NF- κ B P50/P65 activity (n=2 for the Ctrl groups, n=4 for the indicated treatment groups, each lane is an individual rat lung tissue lysate from indicated time point). (B) The intensity of bands was quantified and the Relative NF- κ B P50/P65 activity was plotted.

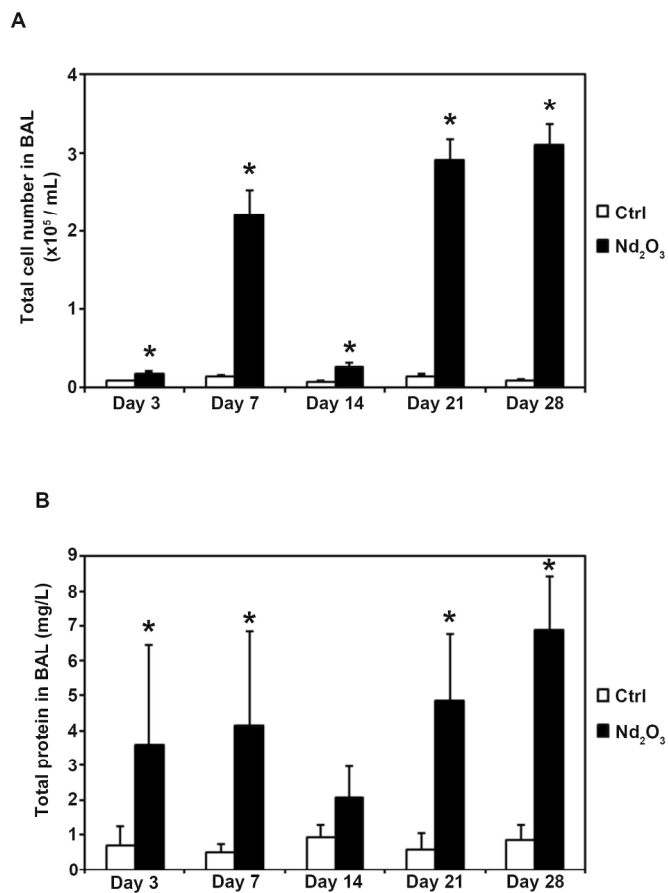
Figure 7. Nd₂O₃ dust intratracheal instillation induced histopathology changes in the lungs of rats along with the activation of NF- κ B signaling pathway in a dose-dependent manner. A1-2, 0 mg/kg; B1-2, 25 mg/kg; C1-2, 50 mg/kg; D1-2, 100 mg/kg; E1-2, 150 mg/kg. A1-E1, 100x; A2-E2, 400x. (n = 7, a representative image of the lung tissue from each group is shown). Scale bar for 100x: 150 μ m; 400x: 40 μ m. (F) Lung tissue lysates from different doses intratracheal instillation rats were subjected to immunoblot analysis with the indicated antibodies (n = 7, each lane is an individual rat lung tissue lysate from indicated dose, and a representative western blot data is shown). (G) The intensity of bands was quantified and the relative ratios of p-P65/P65/ β -actin and p-IKK β / β -actin were plotted. Results are expressed as mean \pm SEM (n = 7) (*p<0.05 control group vs. other doses intratracheal instillation groups).

Figure 1



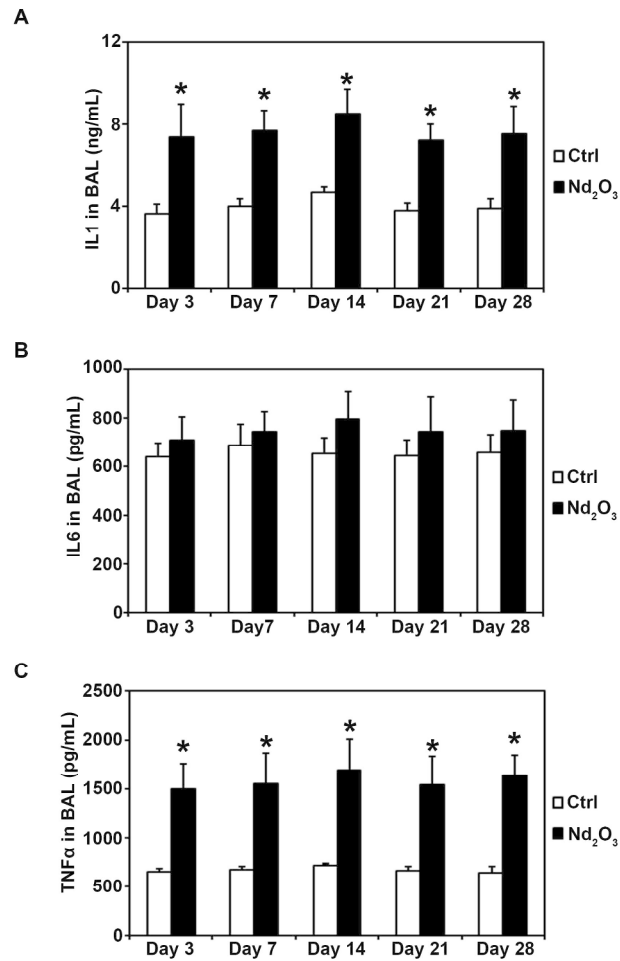
Histopathology changes in the lungs of rats with Nd₂O₃ dust intratracheal (100 mg/kg in PBS) instillation. A1-4, Day 3; B1-4, Day 7; C1-4, Day 14; D1-4, Day 21; E1-4, Day 28. A1-E1, Control group, 100x; A2-E2, Control group, 400x; A3-E3, Nd₂O₃ group, 100x; A4-E4, Nd₂O₃ group, 400x. (n = 7, a representative image of the lung tissue from each group is shown). Scale bar for 100x: 150 μm; 400x: 40 μm. 215x279mm (300 x 300 DPI)

Figure 2



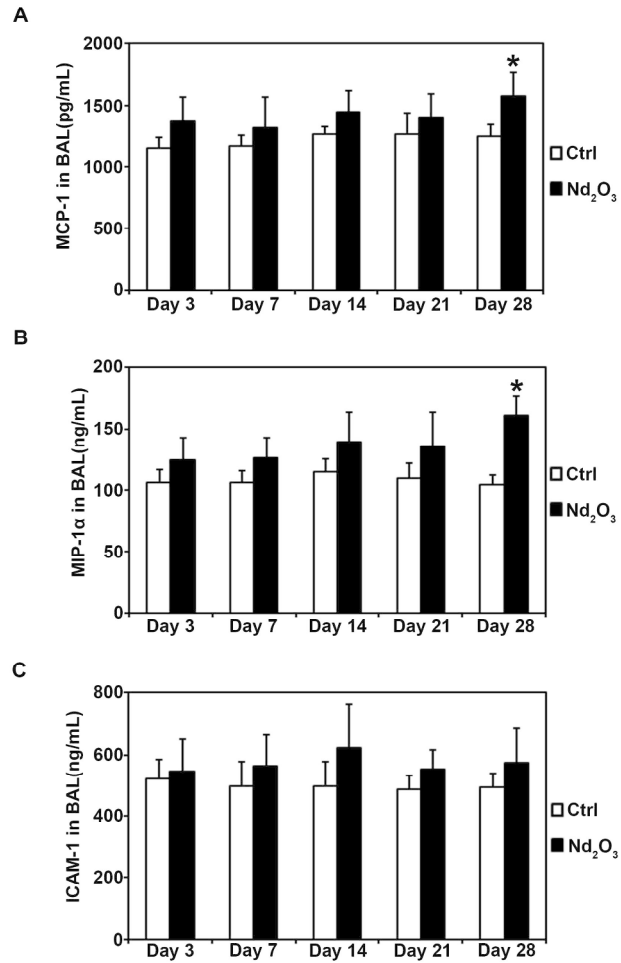
Total cell number and total protein amount in BAL increased in the lungs of rats after rare earth Nd₂O₃ dust intratracheal instillation. (A) Total cell number in BAL; (B) Total protein amount in BAL of the rat lungs harvested from indicated time points.
215x279mm (300 x 300 DPI)

Figure 3



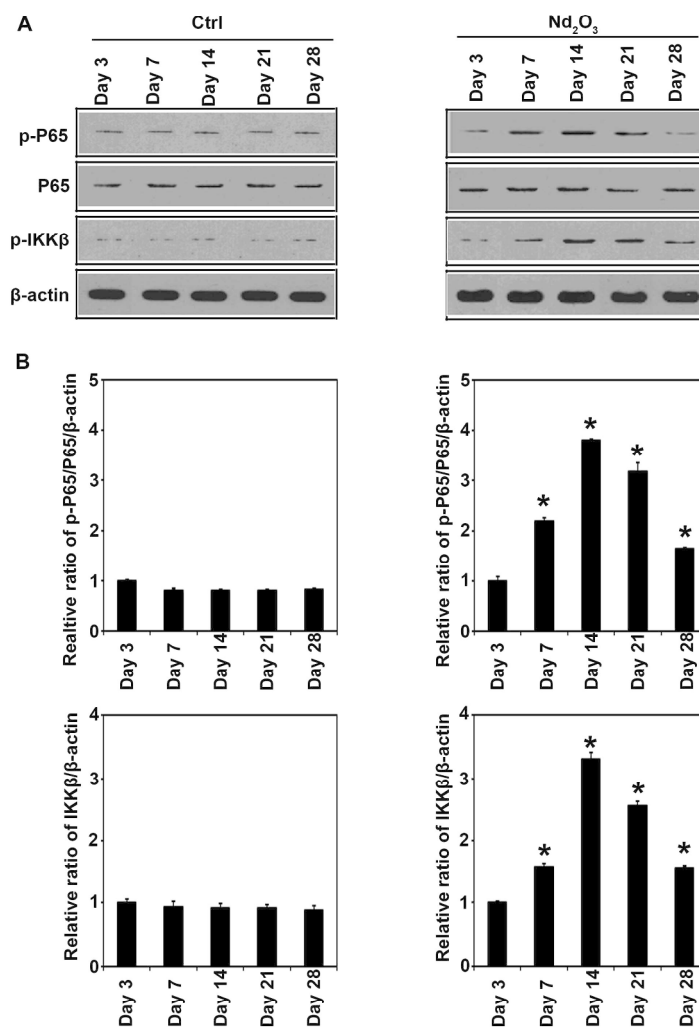
Inflammation cytokines in BAL induced in the lungs of rats with the rare earth Nd₂O₃ dust intratracheal instillation. (A) IL1; (B) IL6; (C), TNF α .
215x279mm (300 x 300 DPI)

Figure 4



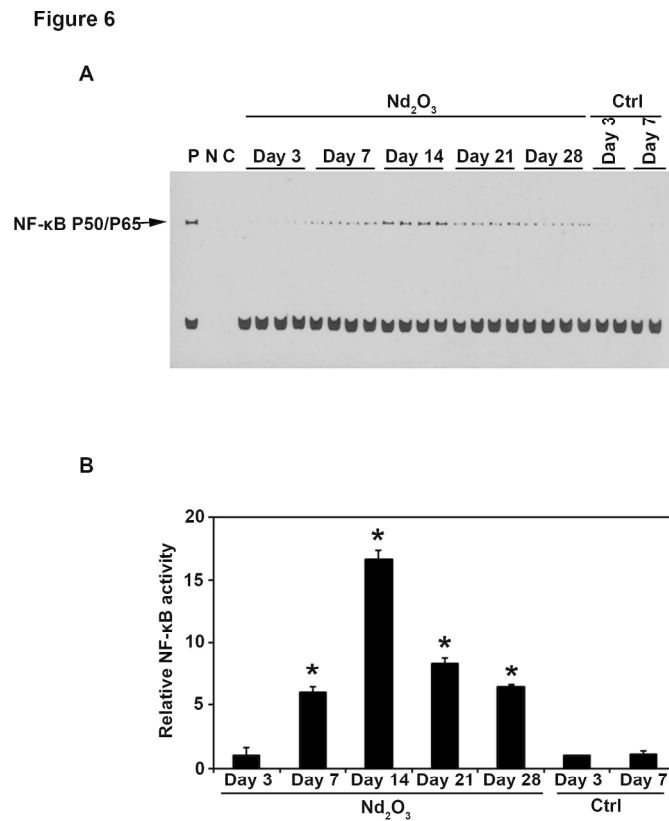
Chemokines in BAL increased in the lungs of rats intratracheally instilled with the rare earth Nd₂O₃ dust. (A) MCP-1; (B) MIP-1 α ; (C) ICAM-1.
215x279mm (300 x 300 DPI)

Figure 5



NF- κ B signaling pathway induced in the lungs of rats with the rare earth Nd₂O₃ dust intratracheal instillation. (A) Lung tissue lysates from Ctrl group rats and Nd₂O₃ rats were subjected to immunoblot analysis with the indicated antibodies ($n = 7$, each lane is an individual rat lung tissue lysate from indicated time point, and a representative western blot data is shown). (B) The intensity of bands was quantified and the relative ratio of p-P65/P65/ β -actin was plotted. Result are expressed as mean \pm SEM ($n = 7$) (* $p < 0.05$ Day 3 group vs. other treatment groups).

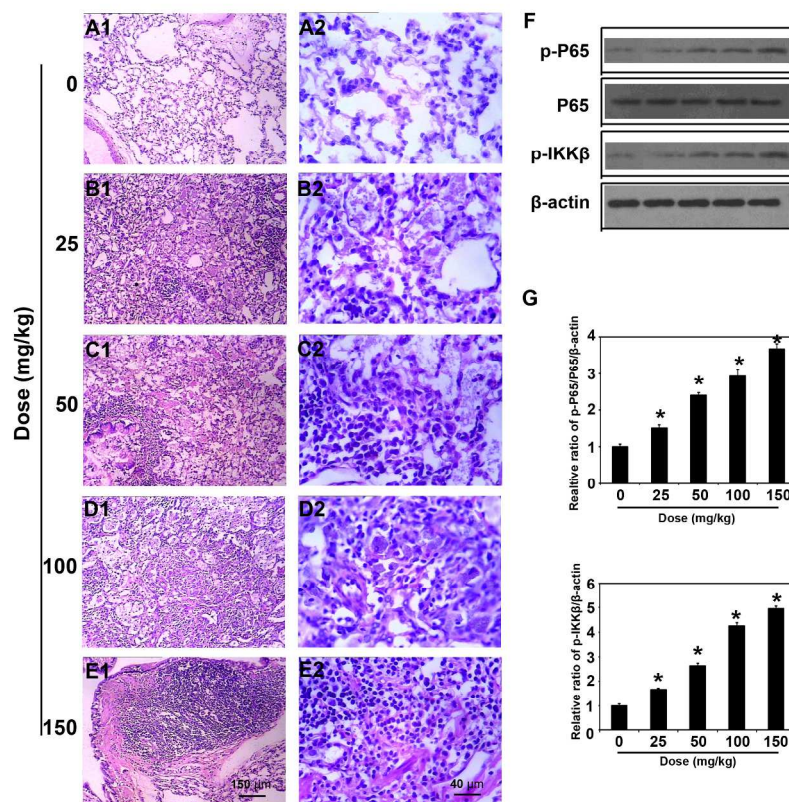
215x279mm (300 x 300 DPI)



NF- κ B P50/P65 activity increased in the lungs of rats administrated with the rare earth Nd₂O₃ dust. (A) Lung tissue lysates from Ctrl groups (Day 3, 7) and Nd₂O₃ groups (Day 3, 7, 14, 21 and 28) were subjected to EMSA assay to detect the NF- κ B P50/P65 activity (n=2 for the Ctrl groups, n=4 for the indicated treatment groups, each lane is an individual rat lung tissue lysate from indicated time point). (B) The intensity of bands was quantified and the Relative NF- κ B P50/P65 activity was plotted.

215x279mm (300 x 300 DPI)

Figure 7



Nd₂O₃ dust intratracheal instillation induced histopathology changes in the lungs of rats along with the activation of NF-κB signaling pathway in a dose-dependent manner. A1-2, 0 mg/kg; B1-2, 25 mg/kg; C1-2, 50 mg/kg; D1-2, 100 mg/kg; E1-2, 150 mg/kg. A1-E1, 100x; A2-E2, 400x. (n = 7, a representative image of the lung tissue from each group is shown). Scale bar for 100x: 150 μm; 400x: 40 μm. (F) Lung tissue lysates from different doses intratracheal instillation rats were subjected to immunoblot analysis with the indicated antibodies (n = 7, each lane is an individual rat lung tissue lysate from indicated dose, and a representative western blot data is shown). (G) The intensity of bands was quantified and the relative ratios of p-P65/P65/β-actin and p-IKKβ/β-actin were plotted. Result are expressed as mean ± SEM (n = 7) (*p < 0.05 control group vs. other doses intratracheal instillation groups).

215x279mm (300 x 300 DPI)

